JOURNAL OF
EMERGING INVESTIGATORS

Article

Strain selective *in vitro* and *in silico* structure activity relationship of tetracycline antibiotics

Alice Zhou[1,2], Shelley Li[1,3], Vivian Long[1,2], Emily Dai[1,2], Lawrence Long[1,2], Edward Njoo[1]

[1] Department of Chemistry, Biochemistry & Physics, Aspiring Scholars Directed Research Program, Fremont, California

[2] BASIS Independent Silicon Valley, San Jose, California

[3] Mission San Jose High School, Fremont, California

SUMMARY

Since the discovery of penicillin G as an effective antibacterial agent by Alexander Flemming in 1928, the demand for new, potent antibiotics has continued to rise due to the development of antibiotic resistance. To combat this crisis, novel antibiotics have been created via optimizing existing structures or natural products found in nature. The tetracycline family of antibiotics is of particular interest due to their broad-spectrum effects. In this study we investigated the antibacterial effects of tetracycline and four of its analogs (chlortetracycline, doxycycline, minocycline, and oxytetracycline) against four species of bacteria. Tetracyclines exhibit bacteriostatic effects by binding to the highly conserved 30S ribosomal subunit of bacteria and interfering in protein synthesis as a result. We hypothesized that the *in vitro* antibacterial efficacy of each tetracycline would vary with each strain and have comparable binding affinities *in silico*. Through Kirby-Bauer disk diffusion assays, we found that the efficacy of those compounds within the tetracycline family was concentration- and strain-dependent. To further elucidate the structure-activity relationship exhibited in the *in vitro* assays, in silico virtual screens were conducted using density functional theory calculations and molecular docking. The computational results demonstrated that all compounds resulted in relatively similar binding affinities, posing a future potential in designing analogs to surpass currently available tetracycline antibiotics.

INTRODUCTION

Tetracyclines, first discovered in the late 1940s, are a unique class of polycyclic natural-product small molecules used for the prophylaxis of human and veterinary infections and even as animal growth promoters (1). Shortly after their discovery and characterization, they were distinguished for their broad-spectrum antibiotic activity against both gram-positive and gram-negative strains, obligate anaerobic bacteria, and protozoan parasites (1). However, despite having over 200 small molecule antibiotics approved by the US Food and Drug Administration (FDA), antibiotic resistance is rapidly increasing among bacterial species (2). The emergence of antibiotic resistance and the growing prevalence of superbugs, strains of bacteria resistant to most antibiotics and common medications, have therefore necessitated the continued development of new antibacterial treatments to match the pace of bacterial evolution (3).

While the first two members of the tetracycline family, oxytetracycline and chlortetracycline, were extracted from the fermentation of *Streptomyces rimosus* and *Streptomyces aureofaciens*, respectively, the majority of second- and third-generation tetracycline analogs were created by the semi-synthesis of various extracts from the *Streptomyces* genus (4). Tetracycline and its analogs have the same basic structure, consisting of a tetracyclic naphthacene carboxamide ring system and various alkyl, hydroxyl, and amine substitutions in upper and lower peripheral zones of the molecule **(Figure 1A)**. Pharmacological properties including bioactivity, stability, and selectivity to intracellular targets are highly dependent on the variable functional groups attached at these R group regions, such as no functional group and hydroxyl and methyl groups **(Figure 1B)** (5). All bioactive tetracyclines that exhibit antibacterial activity must possess a linearly arranged DCBA four-ring system with a C1-C3 diketo substructure and exocyclic C2 carbonyl or amide group. All tetracyclines that function as inhibitors of bacterial protein synthesis also require an amino group at the C4 position (5).

Further research indicated that the mechanism of action for tetracyclines originates from their ability to reversibly bind to the highly conserved bacterial 30S ribosomal subunit, which is made up of 16S rRNA and approximately 20 other proteins (1). Tetracycline mainly binds to its primary site in the subunit, located near the aminoacyl/acceptor site (A site), a decoding location where the anticodons of aminoacyl-tRNA (aa-tRNA) are matched with the codons of mRNA (6). It is predicted that although tetracycline doesn't inhibit the interaction between codon and anticodon and the initiation of decoding, it does sterically hinder the accommodation of aa-tRNA in the A site, preventing protein synthesis from occurring (7). Multiple secondary sites have also been identified for tetracycline within the subunit; however, they are thought to have lower avidity for tetracycline ligands and their relative relevance is still being investigated (7). In this study, we analyzed a secondary site near helix 27, also known as the switch helix, on the 16S rRNA in addition to the primary A site. Unable to directly prohibit tRNA binding at the switch helix, tetracycline likely interferes with the open and closed conformations of the 30S ribosomal subunit that play important roles in the decoding process (8).

Though tetracyclines are highly versatile and potent antibiotics, their overuse has resulted in an increasing number of strains of tetracycline-resistant bacteria. Tetracycline

JOURNAL OF
EMERGING INVESTIGATORS

https://doi.org/10.59720/22-241

A

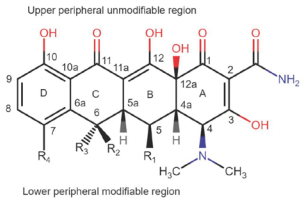

B

Compound	R1	R2	R3	R4
Tetracycline	N/A	CH_3	OH	N/A
Chlortetracycline	N/A	CH_3	OH	Cl
Doxycycline	OH	CH_3	N/A	N/A
Minocycline	N/A	N/A	N/A	$N(CH_3)_2$
Oxytetracycline	OH	CH_3	OH	N/A

Figure 1. A structural analysis on the role of chemical functional groups in tetracycline and its analogs. A) Skeletal formula of tetracycline with atoms and the four fused rings numbered and labeled. The lower peripheral region may be modified or substituted to enhance antibacterial activity, while the upper peripheral region is generally non-modifiable since it is responsible for ion-chelation and anti-metalloproteinase activity to help transport tetracyclines across the cellular membrane (5). **B)** Specific substitutions (N/A = no functional group attached at the region; OH = hydroxyl; CH_3 = methyl; Cl = chloro; $N(CH_3)_2$ = trimethylamine) at the R groups in the lower peripheral region for the five tetracyclines investigated in this study.

resistance is generally attributed to one of a combination of the following developments: 1) efflux, in which bacteria evolve to be equipped with tetracycline-specific efflux pumps to remove the drug from the cytoplasm, 2) enzymatic inactivation of tetracycline drugs that result in the reduction of intracellular and extracellular concentrations of the drugs, or 3) mutations in either the 30S ribosome proteins or 16S rRNA sequence that alter binding affinity and location (9–11). Tetracycline resistance most commonly involves drug efflux pumps, while mutations in the ribosome are not usually attributed to bacterial resistance (7).

Herein, we screened five commonly used and commercially available tetracyclines – tetracycline, chlortetracycline, doxycycline, minocycline, and oxytetracycline – against four species of gram-positive and gram-negative bacteria **(Table 1)**. The bacterial strains subjected to experimentation were *Escherichia coli* and *Serratia marcescens,* which are gram-negative bacteria, and *Brevibacillus brevis* and *Staphylococcus epidermidis*, which are gram-positive bacteria. The antibiotics were tested at concentrations of 5 mM, 1 mM, and 0.2 mM in Kirby-Bauer disk diffusion assays, and the radii of inhibition (ROI) were measured to determine the relative bacteriostatic capabilities of each antibiotic. We conducted both an *in vitro* antimicrobial assay and *in silico* computational modeling to investigate the structure-activity relationship, which is the relationship between chemical structures (tetracycline derivatives) with the biological targets (the bacterial 30S ribosome). Our lab has previously used similar approaches to understand the SAR of other antibiotics, including beta-lactams (12).

We hypothesized that the antibacterial efficacy of each tetracycline would be strain-specific because prior literature indicates that the minimum inhibitory concentration (MIC) value of each compound varies when tested against different bacterial strains (13). The results were consistent with the hypothesis and showed that some tetracyclines are better equipped to inhibit the growth of certain bacterial strains. In addition, we predicted that the screened tetracycline compounds would perform comparatively *in silico*. The resulting binding affinities supported this as well, since the semi-synthesized derivatives only enhance abilities to cross membranes or resist efflux proteins (1, 14). Our conclusions may provide background for future synthesis of tetracycline analogs to combat antibacterial resistance.

Compound	Structure	Trade Name
Tetracycline	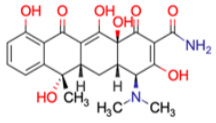	Sumycin, Actisite
Chlortetracycline	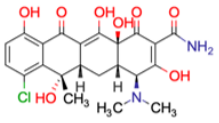	Aureomycin
Doxycycline	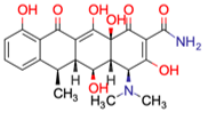	Vibramycin, Doryx
Minocycline	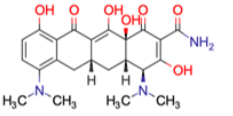	Dynacin, Minocin
Oxytetracycline	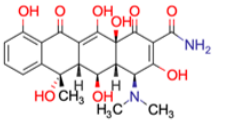	Terramycin

Table 1. Tetracycline family antibiotics. The antibiotics shown are commercially available and clinically approved to combat mycobacterial infections.

RESULTS

In vitro assays

We determined relative effectiveness of each tetracycline antibiotic through Kirby-Bauer assays **(Figure 2)**. We placed antibiotic disks on petri dishes, inhibiting bacterial growth circularly around the disk. The extent to which the bacterial growth is inhibited is directly correlated to antibiotic efficiency, measured by calculating the ROI, with greater ROI correlated to more potent bacteriostatic activity (15). After culturing both gram-negative *E. coli* and *S. marcescens* and gram-positive *B. brevis* and *S. epidermis*, the bacteria were exposed

https://doi.org/10.59720/22-241

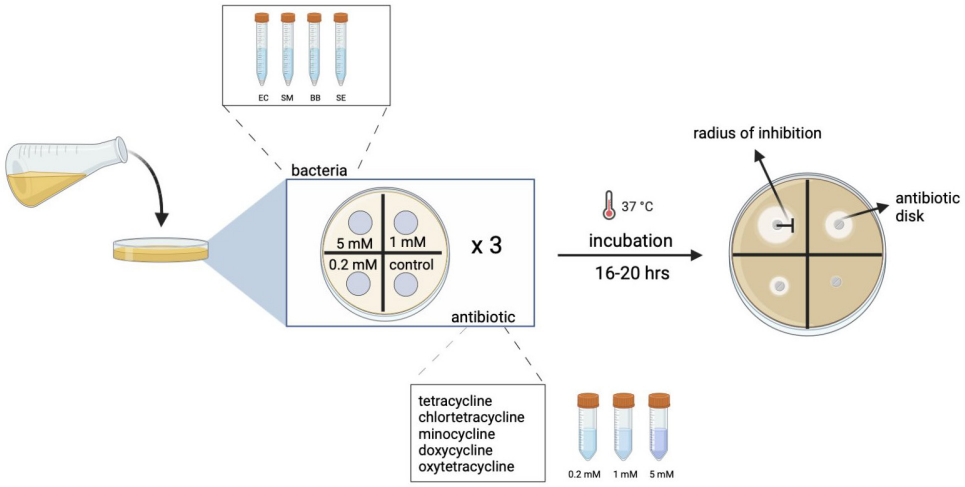

Figure 2. Kirby-Bauer assay experimental setup. Petri dishes were divided into four groups of fifteen dishes for each bacterial strain, and further divided into quadrants which held a different concentration of each antibiotic. The assay was conducted in triplicate, with each combination of bacteria, antibiotic, and concentration replicated on three dishes. Bacteria was streaked across each petri dish, and a 6 mm filter paper disk with the appropriate concentration of the antibiotic or deionized water was placed in each quadrant. Agar plates were incubated for 16-20 hours at 37°C before the radius of inhibition was measured. Created with BioRender.com.

to different concentrations of each of the five tetracycline compounds. ROI was measured for all trials and three trials were performed.

Across all the antibiotic-bacteria pairs, we observed dose-dependent activity, in which a five-fold increase in antibiotic concentration led to an increase in ROI. However, while trends in concentration were uniform across bacteria strains and antibiotics, the strain-specific antibacterial efficacy varied in all cases.

EC was susceptible to all tetracyclines, but oxytetracycline was the most successful in preventing EC growth with the largest mean ROI among the other tetracyclines in all three concentrations. Across the five tetracyclines, the ROI ranged from 14.5 - 17.4 mm at 5 mM, 12 - 14.4 mm at 1 mM, and 7.7 - 11.4 mM at 0.2 mM, with oxytetracycline, minocycline, and chlortetracycline performing comparably **(Figure 3A)**. However, Tukey HSD tests (α of 0.05) showed that although both minocycline and chlortetracycline showed no significant difference in ROI with oxytetracycline at 5 mM (p=0.59 and p=0.43, respectively), they had significantly lower ROI when compared to oxytetracycline at 0.2 mM for minocycline and 1 mM for chlortetracycline.

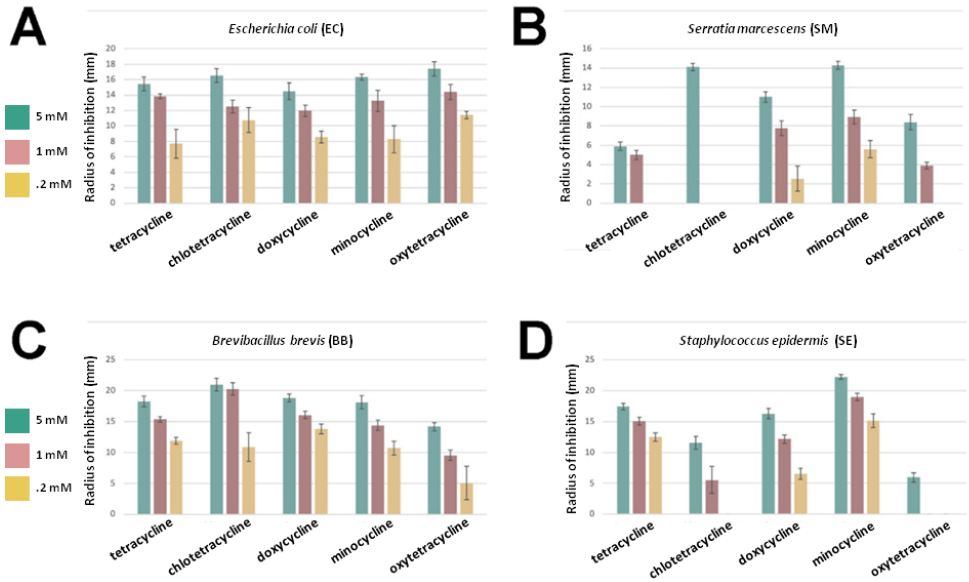

Figure 3. Antibiotic efficacy was concentration- and strain-specific. Average radius of inhibition of five tetracycline compounds (tetracycline, chlortetracycline, doxycycline, minocycline, and oxytetracycline) at three different concentrations (5mM: green bar, 1mM: red bar, and 0.2mM: yellow bar) for four species of bacteria: **A)** *Escherichia coli,* **B)** *Serratia marcescens,* **C)** *Brevibacillus brevis*, **D)** *Staphylococcus epidermidis*. Data shown as mean ± 2 SEM,, each combination was replicated three times. One-way ANOVA and Tukey HSD tests (α of 0.05) were conducted to determine statistical significance.

https://doi.org/10.59720/22-241

All our tetracycline analogs performed poorly against *S. marcescens* with ROIs ranging from 5.9 - 14.3 mm for 5 mM concentration, 0 - 8.9 mm for 1 mM concentration, and 0 - 5.6 mm for 0.2 mM concentration **(Figure 3B)**. Overall, the second generation, semi-synthesized doxycycline and minocycline inhibited bacterial growth better than oxytetracycline and tetracycline, being able to prohibit bacterial growth at 0.2mM, while the latter two could not. In addition, although chlortetracycline demonstrated comparable antibacterial properties when applied at 5 mM concentration and displayed no significant difference in mean ROI when compared with that of 5 mM minocycline in the Tukey HSD test (α of 0.05) (p=0.99), it was unable to prevent SM growth at any lower concentration.

Against the gram-positive strain *B. brevis*, chlortetracycline had the greatest mean ROI of 21 mm and 20.3 mm at 5 mM and 1 mM, respectively. At 0.2 mM, most of our the tetracyclines tested demonstrated similarly high levels of inhibition **(Figure 3C)**. Tukey HSD tests (α of 0.05) revealed that there was no significant difference in mean ROI between tetracycline (11.9 mm) and chlortetracycline (10.9 mm), doxycycline (13.8 mm), and minocycline (10.7 mm) (p=0.92, p=0.54, p=0.87, respectively compared to tetracycline), indicating that at low concentrations, BB is highly susceptible to most of our tested tetracycline compounds. Even doxycycline, which consistently performed the worst at all three concentrations, had an average 5.1 mm ROI at 0.02 mM.

Nevertheless, against the second gram-positive bacteria used in this study, SE, doxycycline outperformed both oxytetracycline and chlortetracycline, which were unable to hinder bacterial growth at 1 mM and 0.2 mM, respectively **(Figure 3D)**. In addition, minocycline had the greatest mean ROI of all tetracyclines in all three concentrations at 22.2 mm (5 mM), 19mm (1 mM), and 15.2 mm (0.2 mM) against *S. epidermis*.

For all tetracyclines, there were significant differences in antibacterial efficacy among the four strains when compared using a one-way ANOVA with Tukey HSD post-hoc test. Tetracycline was most effective against BB and SE (p=1.4*10^{-22}). Chlortetracycline had the greatest ROI against BB (p=4.4*10^{-15}), but at 0.02 mM, performed equally effectively against EC (p=0.10). Oxytetracycline demonstrated the highest levels of bacterial inhibition against EC (p=7.2*10^{-20}), doxycycline against BB (p=6.5*10^{-14}), and minocycline against SE (p=6.3*10^{-17}).

In silico analysis

To provide structural and computational insight in the SAR observed in our Kirby-Bauer assays, molecular docking of the five tetracycline compounds was performed. The structures of the antibiotics were first geometrically optimized using density functional theory (DFT) calculations to obtain the most stable structure and lowest energy state (**Figure 4A**). Then, they were docked to a primary binding site near the A site of the 30S ribosomal subunit and a secondary site next to switch helix 27, both of which are important to protein synthesis and specifically, the decoding of amino acids **(Figure 4B)**. Different binding modes or conformations of the bound ligand-receptor (1: lowest binding affinity; 9: highest binding affinity) were chosen to mimic the closest binding position to that reported in literature and observed crystallographically, with the hydrophilic side of tetracycline facing the 16S rRNA (7). The root mean standard deviation (RMSD) was then measured with the docked and the experimental structure of the ligand **(Table 2)**. The tetracycline ligand within the 30S ribosomal subunit [PDB:1HNW] was also redocked to validate docking parameters and served as a control.

In the primary binding site, the tetracycline compounds mainly interacted with the phosphate backbone of helix 34 or RNA residues 1195-1200 through hydrogen bonds between carbonyl or hydroxyl oxygen atoms on the tetracycline scaffold and the phosphate oxygens on the phosphate backbone **(Figure 5)**. On the nonmodifiable hydrophilic side of the tetracyclines, hydroxyl groups at the 10, 12, and 12a positions formed hydrogen bonds with guanine 1197 and 1198 as well as cytosine 1054. The strong binding affinities of chlortetracycline and doxycycline can be attributed to binding positions closer to cytosine 1054 that allowed the position 10 hydroxyl to bind closely with the nitrogen (approximately 2.5 Å) and oxygen (approximately 3 Å) on residue 1054. On the other hand, oxytetracycline was too far to make any contacts, and position 10 hydroxyls on minocycline and tetracycline bound to both oxygen and nitrogen of cytosine 1054 at an average distance of 3 Å. Nevertheless, because minocycline and tetracycline were farther away from residue 1054, their position 12 hydroxyl was able to form three rather than one hydrogen bond (which was the case for the other three tetracyclines) with the oxygens on the phosphate of guanine 1198 and 1197. Notably, minocycline's larger size also enabled it to reach guanine 966 on neighboring helix 31 and form a hydrogen bond 2.22 Å away. In addition, although oxytetracycline made spare interactions at both 10 and 12 positions, its position 12a hydroxyl formed the most interactions of three hydrogen bonds: two bonds with oxygens on the phosphate of guanine 1198 at distances of 2.15 Å and 2.66 Å and one bond with the 3' hydroxyl on guanine 1197 at 2.83 Å.

For all the tetracyclines, the amino group also made crucial contacts with the oxygens on the phosphates in cytosine 1195 and uracil 1196. Because the A ring for tetracycline and chlortetracycline was closer to the two residues, those two compounds formed three hydrogen bonds at average distances of 2.9 Å, while the other tetracyclines had only one or two farther hydrogen bonds.

In our results, tetracycline minimized the distance with magnesium the best; its β-diketone system (positions 11 and 12) interacted with the metal ion at distances of 2.31 Å and 2.68 Å, contributing to the ligand's strong binding affinity.

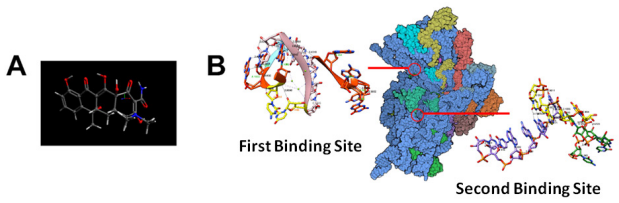

Figure 4. Molecular docking of tetracycline compounds into primary and secondary binding sites of 30S ribosomal subunit. A) Geometrically optimized structure of tetracycline. **B)** The primary site is bordered by helix 34 (residues 1195-1200) and helix 31 (residues 964-967), while the secondary binding site consists of helix 27 (residues 891-894, 906-911) and helix 11 (residues 242-245) on the 30S ribosomal subunit [PDB: 1HNW]. Created with BioRender.com and UCSF Chimera Version 1.16 (2021-12-17).

https://doi.org/10.59720/22-241

	control	tetracycline	chlor-tetracycline	oxy-tetracycline	doxycycline	minocycline
Primary Binding Site Affinity (kcal/mol)	-5.8	-5.7	-6.0	-5.5	-5.8	-5.4
RMSD (Å)	0.577	0.443	0.728	0.665	0.676	0.795
Secondary binding site affinity (kcal/mol)	-5.4	-6.9	-7.3	-7.9	-7.6	-6.5
RMSD (Å)	0.551	0.674	0.616	0.488	1.007	0.802

Table 2. Binding affinity, the binding mode chosen, and RMSD of tetracycline compounds bound to primary and secondary binding sites in the 30S ribosomal subunit.

When binding to the secondary binding site, rather than to the phosphate backbone, the tetracyclines were mainly bound to the exposed ribose **(Figure 6)**. The binding pocket was made of helix 27 (residues 891-894, 906-911) and helix 11 (residues 242-245). Most of the hydrogen bonding occurred between the nitrogen and oxygens on the A ring of tetracyclines and oxygens on the sugar moieties. At positions 12 and 12a, all tetracyclines had hydrogen bonds between their hydroxyls and residues 892, 893, 907, and 244. Oxytetracycline formed the most hydrogen bonds at position 12, interacting with the nitrogen and oxygen on uracil 244 at 3 Å and 2.23 Å respectively, as well as cytosine 893 at 2.59 Å. Additionally, at position 12a, minocycline had the most contacts at four hydrogen bonds: three with adenine 907 at an average distance of 3.2 Å each, and one with cytosine 892 at 2.8 Å.

Chlortetracycline and doxycycline were the only two compounds that contained hydroxyls at position 10 that interacted with the 3' hydroxyl on guanine 906, forming hydrogen bonds at 3.03 Å and 2.46 Å respectively. On the other hand, tetracycline was the only one with no interaction at position 1, and minocycline, the only one with no interaction at position 11, which weakened their respective binding affinities. Moreover, while the other four tetracyclines did comparably at position 1, at position 11, chlortetracycline performed the best with two instead of one hydrogen bond at an average distance of 3 Å. In addition, out of all the tetracyclines, oxytetracycline had the strongest binding affinity, likely because it was the only one that formed a hydrogen bond with adenine 907 at the position 5 hydroxyl, and it had the closest hydrogen bond between the position 6 hydroxyl and uracil 244 at a distance of 2.71 Å.

The second binding site didn't have a magnesium ion to facilitate or enhance the binding of tetracyclines to the binding site; however, it did have interactions between uracil 244 and cytosine 893 that connected the two helices and knitted the binding pocket together. Both tetracycline and minocycline, which had weak binding affinities, had multiple hydrogen bonds at the amino group, mainly with uracil 244, cytosine 893, and guanine 894. Chlortetracycline and tetracycline didn't have bonds at the amino group, and doxycycline only formed hydrogen bonds with residues on helix 11—uracil 244 and cytosine 245.

Overall, binding affinities were comparable, with little variation, especially for the primary binding site. This may have occurred because the magnesium ions restricted the ligands in finding significantly better binding positions; in their absence in the secondary binding site, certain tetracycline compounds were able to demonstrate more variance and higher binding affinities.

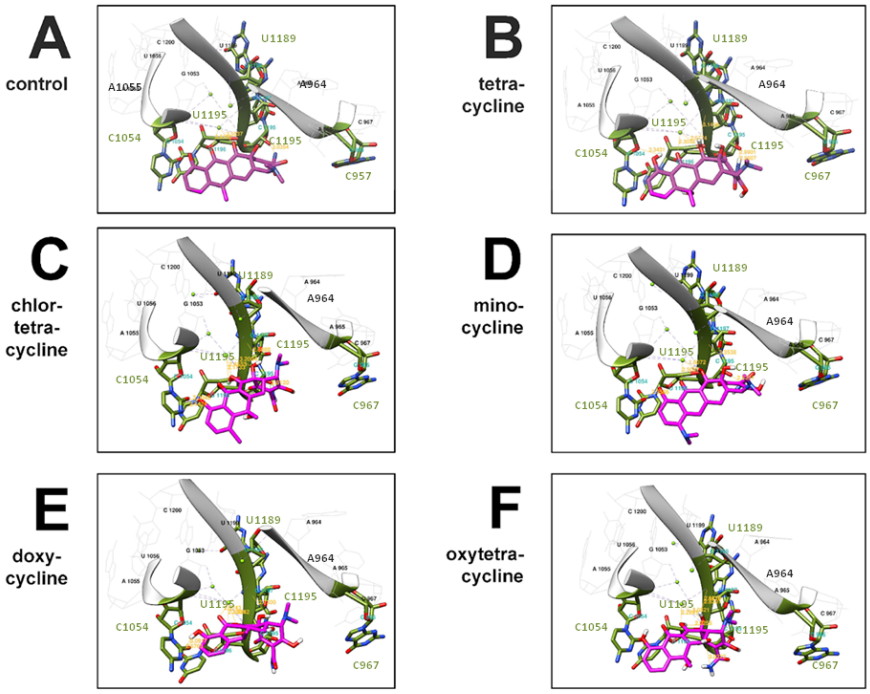

Figure 5. Tetracycline compounds within the primary binding site. A) Binding of control (innate ligand within PDB 1HNW) to primary binding site, **B)** Binding of tetracycline to primary binding site, **C)** Binding of chlortetracycline to primary binding site, **D)** Binding of minocycline to primary binding site, **E)** Binding of doxycycline to primary binding site, **F)** Binding of oxytetracycline to primary binding site. Purple dotted lines are contacts such as salt bridges that magnesium ions form with the binding pocket; yellow lines and numbers represent some of the interactions between ligands (magenta) and RNA residues 1195-1198 and 1054 (green). Created with UCSF Chimera Version 1.16 (2021-12-17).

https://doi.org/10.59720/22-241

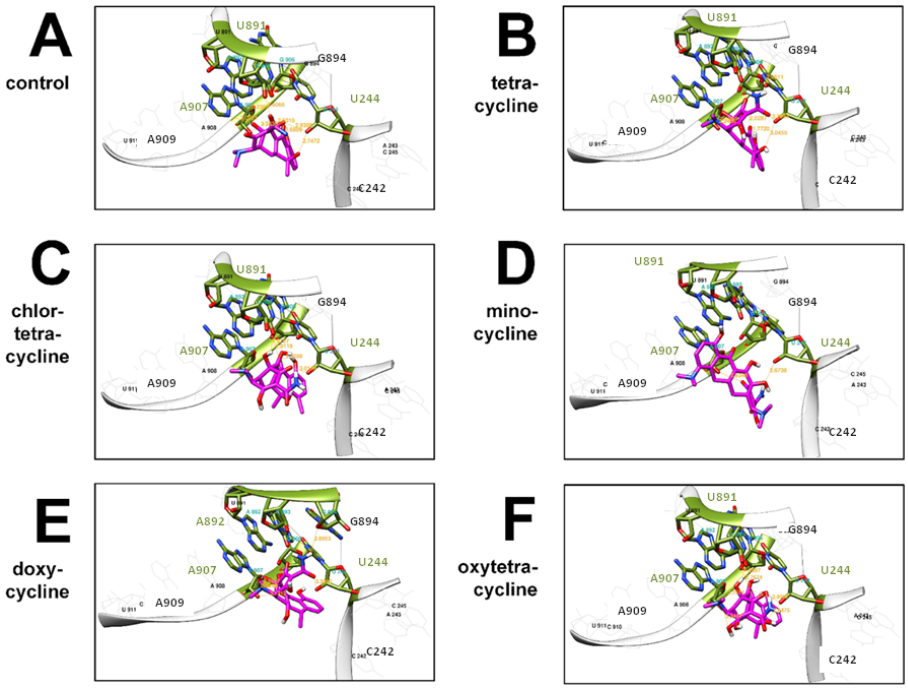

Figure 6. Tetracycline compounds within the secondary binding site. A) Binding of control (tetracycline ligand within the 30S ribosomal subunit [PDB:1HNW]) to secondary binding site, **B)** Binding of tetracycline to secondary binding site, **C)** Binding of chlortetracycline to secondary binding site, **D)** Binding of minocycline to secondary binding site, **E)** Binding of doxycycline to secondary binding site, **F)** Binding of oxytetracycline to secondary binding site. Yellow lines and numbers represent some of the hydrogen bonds between ligands (magenta) and RNA residues 244, 904, 906, 907, 892, and 893 (green). Created with UCSF Chimera Version 1.16 (2021-12-17).

DISCUSSION

Tetracyclines are believed to enter gram-negative bacteria as either positively charged magnesium-tetracycline complexes or ionically bonded to magnesium ions, which then dissociate into a weak lipophilic molecule to diffuse into the inner membrane (1). The other gram-negative bacteria, SM, is known to exhibit high resistance to tetracyclines and has been isolated before from heavily contaminated heavy metals (16, 17). In gram-positive bacteria, tetracyclines are also known to travel across the cytoplasmic membrane in a lipophilic form; however, rather than positively charged cations, the complex transferred across carries no net electric charge (18). Designed with greater liposolubility, minocycline and doxycycline are better able to enter gram-positive bacteria than first-generation tetracyclines; thus, their heightened antibacterial inhibition was likely due to their ability to traverse cytoplasmic membranes more smoothly (13).

Although tetracyclines are well-established and effective antibiotic treatments, the development of antibiotic resistance heightens the demand for new bacterial protein synthesis inhibitors. As second-generation drugs, minocycline and doxycycline are generally more advantageous antibiotics when compared to chlortetracycline, oxytetracycline, and tetracycline due to their greater lipophilicity and gastrointestinal and oral absorption (22, 23). However, while doxycycline and minocycline did perform best overall in our *in vitro* screening, showing inhibition for all concentrations and strains, outperformance in BB and EC by other tetracyclines supported our hypothesis that the bacteriostatic activity of the tested antibiotics was strain- and concentration-dependent. Furthermore, in our supporting *in silico* studies, which predict the drug's abilities to bind in the binding pocket and thus, the effectiveness of the drug, all the tetracyclines had comparable binding affinities as per our hypothesis.

Although the use of computation methods to mimic biological processes saves both the money and time needed to conduct intensive *in vitro* or *in vivo* studies, there are many limitations to the accuracy of docking software like Autodock Vina. There are also two reported crystal structures for the 30S subunit of *Thermus thermophilus*, one with two binding sites for tetracycline [PDB:1HNW] and the other, six [PDB:1I97] (7, 24). Due to the uncertainty of the functional relevance and the lack of biochemical data for the binding of tetracycline to the latter's secondary sites, we chose to use the former crystal structure (6, 7). Nevertheless, the presence of two structures with different binding sites does introduce an element of uncertainty into our investigation. In addition, the use of the crystal structure of the 30S subunit of *Thermus thermophilus*, an extremophile, for studying tetracycline binding sites and mechanisms within bacteria is prevalent, especially the binding sites in the highly conserved 16S rRNA. Tetracyclines are known to bind to magnesium in the primary binding site (7). Tetracyclines are strong chelating agents, and their antibacterial properties are impacted by their binding with metal ions (19). For example, the presence of magnesium ions has been shown to impact the frequency of tetracyclines binding to nucleic acids in the binding pocket as well as enhance the interaction of tetracyclines with double-stranded RNAs (20, 21). However, studies indicating a more densely packed thermophilic 16S ribosomal RNA in *T. thermophilus* compared to EC does suggest structural differences from the bacteria tested in our *in vitro* experiments (6, 7, 12, 25-28). The docking with the presence of magnesium may have

https://doi.org/10.59720/22-241

also impacted the ligands' ability to find more optimal binding positions. Given the joined binding site, when the amino group on the tetracyclines formed additional interactions with both helices, it most likely tightened the binding space, resulting in steric issues.

Future research may investigate the effect of mutations in the 30S subunit on various tetracyclines as well as the design of analogs, such as novel synthetic modifications to the D-ring, in order to optimize the performance of this family of antibiotics to combat the growing prevalence of antibacterial resistance. Such studies are underway in our laboratory and shall be reported in the future.

MATERIALS AND METHODS

Kirby-Bauer disk diffusion assay

The Kirby-Bauer assay was used to measure the resistance of different bacteria strains to tetracycline and its analogs. Mueller-Hinton agar was prepared following standard protocols and poured into petri dishes to cool under a sterile laminar flow hood.

The petri dishes were split into four groups with fifteen dishes for each bacteria. The assay was conducted in triplicate for each antibiotic at concentrations of 5 mM, 1 mM, and 0.2 mM against two strains of gram-positive and two strains of gram-negative bacteria. Each dish was divided into four quadrants of varying concentrations of antibiotic (tetracycline, chlortetracycline, minocycline, doxycycline, and oxytetracycline). Bacteria was then streaked across each petri dish, and a 6 mm filter paper disk impregnated with the appropriate concentration of the antibiotic or deionized water was placed in each quadrant. The agar plates were incubated for 16-20 hours at 37°C before the radius of inhibition was measured via calipers, and the ROI was calculated.

To compare the effects of different strains of bacteria on the ROI of the tetracycline compounds, one-way ANOVA and Tukey HSD post-hoc tests (α of 0.05) were conducted with the data.

Molecular-Mechanical (MM) optimization (Avogadro)

The tetracycline compound family was created using Avogadro (Version 1.2.0), an advanced molecule editor and visualizer used in molecular modeling (29). Using molecular mechanics, all of the molecules were optimized with the UFF94 force field at 10,000 steps.

Density functional theory (DFT)

To optimize the geometries and minimize the energies of the tetracycline structures, DFT calculations were done with Avogadro, Open Babel, and ORCA (29-31). Avogadro was used to create DFT input files, and Open Babel was used to find the lowest conformer form. The calculations were then performed using ORCA, an *ab initio* quantum chemical modeling suite, with a B3LYP functional, 6-31g basis set, and implicit solvation in water.

Molecular docking

Using Autodock Vina 1.5.7, tetracycline, chlortetracycline, minocycline, oxytetracycline, and doxycycline, were docked into the primary and secondary binding site within the unliganded structure of the 30S ribosomal subunit [PDB:1HNW]. For the primary binding site, the coordinates of the center atom were 205.502, 109.132, and 4.235, and for the second binding site, 160.296, 80.686, and -21.986, with a gridbox of dimensions 10 Å by 10 Å by 10 Å for both. Exhaustiveness was increased to 100, and the crystal and experimental structures of the tetracyclines were redocked into both binding sites to validate docking parameters. Autodock Vina calculated binding affinities of nine docking modes, and the binding mode most consistent with the observed crystallographic pose (hydrophilic side of tetracycline facing the 16S rRNA) was chosen (7, 32). Due to limitations of modeling programs such as Autodock Vina, the chosen mode was not always the most favorable binding mode (lowest binding affinity). Although docking generates many potential candidates for high binding affinities, the low computational cost of molecular docking implies many approximations made in the process (33). Docking results were then analyzed with UCSF Chimera Version 1.16 (2021-12-17) to visualize the ligand-bound binding pocket and measure the distances of hydrogen bonds between key residues and compounds (34). The root-mean-square deviation (RMSD) between the experimental structures and the docked ligand was computed via PyMOL (35).

All docking was conducted on a Dell PowerEdge 710 server with a 24-core Intel Xeon X5660 processor at 2.80 GHz and 32 GB RAM.

ACKNOWLEDGEMENTS

We would like to thank the ASDRP Chemistry and Computer Science Department for the allocation of materials and funding for our research.

Received: October 7, 2022
Accepted: April 2, 2023
Published: July 20, 2025

REFERENCES

1. Chopra, Ian, and Marilyn Roberts. "Tetracycline Antibiotics: Mode of Action, Applications, Molecular Biology, and Epidemiology of Bacterial Resistance." *Microbiology and Molecular Biology Reviews*, vol. 65, no. 2, 1 June 2001, pp. 232–260. https://doi.org/10.1128/mmbr.65.2.232-260.2001.
2. Ribeiro da Cunha, et al. "Antibiotic Discovery: Where Have We Come from, Where Do We Go?" *Antibiotics*, vol. 8, no. 2, 24 Apr. 2019, p. 45. https://doi.org/10.3390/antibiotics8020045.
3. Sengupta, Saswati, et al. "The Multifaceted Roles of Antibiotics and Antibiotic Resistance in Nature." *Frontiers in Microbiology*, vol. 4, 12 Mar. 2013. https://doi.org/10.3389/fmicb.2013.00047.
4. Wang, Xuefeng et al. "Heterologous production of chlortetracycline in an industrial grade Streptomyces rimosus host." *Applied Microbiology and Biotechnology*, vol. 103, no. 16, Aug. 2019, pp. 6645-6655. https://doi.org/10.1007/s00253-019-09970-1.
5. Fuoco, Domenico. "Classification Framework and Chemical Biology of Tetracycline-Structure-Based Drugs." *Antibiotics*, vol. 1, no. 1, 12 June 2012, pp. 1–13. https://doi.org/10.3390/antibiotics1010001.
6. Chukwudi, Chinwe U. "RRNA Binding Sites and the Molecular Mechanism of Action of the Tetracyclines." *Antimicrobial Agents and Chemotherapy*, vol. 60, no. 8, 22 July 2016, pp. 4433–4441. https://doi.org/10.1128/

aac.00594-16.
7. Brodersen, Ditlev E., et al. "The Structural Basis for the Action of the Antibiotics Tetracycline, Pactamycin, and Hygromycin B on the 30S Ribosomal Subunit." *Cell*, vol. 103, no. 7, 22 Dec. 2000, pp. 1143–1154. https://doi.org/10.1016/s0092-8674(00)00216-6.
8. Connell, Sean R., et al. "Ribosomal Protection Proteins and Their Mechanism Of Tetracycline Resistance." *Antimicrobial Agents and Chemotherapy*, vol. 47, no. 12, Dec. 2003, pp. 3675–3681. https://doi.org/10.1128/aac.47.12.3675-3681.2003.
9. Wang, Weixia, et al. "High-Level Tetracycline Resistance Mediated by Efflux Pumps Tet(a) and Tet(a)-1 with Two Start Codons." *Journal of Medical Microbiology*, vol. 63, no. 11, 2014, pp. 1454–1459. https://doi.org/10.1099/jmm.0.078063-0.
10. Oehler, R. "Interaction of Tetracycline with RNA: Photoincorporation into Ribosomal RNA of Escherichia Coli." *Nucleic Acids Research*, vol. 25, no. 6, 1997, pp. 1219–1224. https://doi.org/10.1093/nar/25.6.1219.
11. Trieber, Catharine A., and Diane E. Taylor. "Mutations in the 16S Rrna Genes of *Helicobacter Pylori* Mediate Resistance to Tetracycline." *Journal of Bacteriology*, vol. 184, no. 8, 2002, pp. 2131–2140. https://doi.org/10.1128/jb.184.8.2131-2140.2002.
12. Poosarla, Ayeeshi, et al. "Strain-Selective in Vitro and in Silico Structure Activity Relationship (SAR) of N-Acyl β-Lactam Broad Spectrum Antibiotics." *Journal of Emerging Investigators*, vol. 4, 19 Oct. 2021, pp. 1–9.
13. Grossman, Trudy H. "Tetracycline Antibiotics and Resistance." *Cold Spring Harbor Perspectives in Medicine*, vol. 6, no. 4, 17 Apr. 2016. https://doi.org/10.1101/cshperspect.a025387.
14. Mercer, Melissa A. "Tetracyclines Use in Animals - Pharmacology." *Merck Veterinary Manual*, 13 June 2023. www.merckvetmanual.com/pharmacology/antibacterial-agents/tetracyclines. Accessed 19 June 2023.
15. Smilack, Jerry D. "The Tetracyclines." *Mayo Clinic Proceedings*, vol. 74, no. 7, 1999, pp. 727-729. doi.org/10.4065/74.7.727.
16. Siboni, K. "Sensitivity of Serratia to Tetracycline." *Acta Pathologica Microbiologica Scandinavica Section B Microbiology*, vol. 88B, no. 1-6, 2009, pp. 189–192. https://doi.org/10.1111/j.1699-0463.1980.tb02627.x.
17. Thompson, Stuart A., et al. "Novel Tetracycline Resistance Determinant Isolated from an Environmental Strain of *Serratia Marcescens*." *Applied and Environmental Microbiology*, vol. 73, no. 7, 16 Feb. 2007, pp. 2199–2206. https://doi.org/10.1128/aem.02511-06.
18. McMurry, L M, et al. "Active Uptake of Tetracycline by Membrane Vesicles from Susceptible Escherichia Coli." *Antimicrobial Agents and Chemotherapy*, vol. 20, no. 3, Sept. 1981, pp. 307–313. https://doi.org/10.1128/aac.20.3.307.
19. Chopra, I., et al. "Tetracyclines, Molecular and Clinical Aspects." *Journal of Antimicrobial Chemotherapy*, vol. 29, no. 3, Mar. 1992, pp. 245–277. https://doi.org/10.1093/jac/29.3.245.
20. Noah, James W., et al. "Effects of Tetracycline and Spectinomycin on the Tertiary Structure of Ribosomal RNA in the Escherichia Coli 30 S Ribosomal Subunit." *Journal of Biological Chemistry*, vol. 274, no. 23, 4 June 1999, pp. 16576–16581. https://doi.org/10.1074/jbc.274.23.16576.
21. Chukwudi, Chinwe U, and Liam Good. "Interaction of the Tetracyclines with Double-Stranded RNAS of Random Base Sequence: New Perspectives on the Target and Mechanism of Action." *The Journal of Antibiotics*, vol. 69, no. 8, 20 Aug. 2016, pp. 622–630. https://doi.org/10.1038/ja.2015.145.
22. Garrido-Mesa, N et al. "Minocycline: far beyond an antibiotic." *British journal of pharmacology*, vol. 169, no. 2, 2013, pp. 337-52. https://doi.org/10.1111/bph.12139.
23. Holmes, Natasha E. "Safety and Efficacy Review of Doxycycline." *Clinical Medicine: Therapeutics*. https://doi.org/10.4137/CMT.S2035.
24. Pioletti, M. "Crystal Structures of Complexes of the Small Ribosomal Subunit with Tetracycline, Edeine and IF3." *The EMBO Journal*, vol. 20, no. 8, 17 Apr. 2001, pp. 1829–1839. https://doi.org/10.1093/emboj/20.8.1829.
25. Anokhina, Maria M et al. "Mapping of the second tetracycline binding site on the ribosomal small subunit of E.coli." *Nucleic acids research* vol. 32, no. 8, 11 May. 2004, pp. 2594-2597. https://doi.org/10.1093/nar/gkh583.
26. Cocozaki, Alexis I et al. "Resistance mutations generate divergent antibiotic susceptibility profiles against translation inhibitors." *Proceedings of the National Academy of Sciences of the United States of America*, vol. 113, no. 29, 2016, pp. 8188-8193. https://doi.org/10.1073/pnas.1605127113.
27. Jenner, Lasse et al. "Structural basis for potent inhibitory activity of the antibiotic tigecycline during protein synthesis." *Proceedings of the National Academy of Sciences of the United States of America*, vol. 110, no. 10, 2013, pp. 3812-3816. https://doi.org/10.1073/pnas.1216691110.
28. Mallik, Saurav, and Sudip Kundu. "A comparison of structural and evolutionary attributes of Escherichia coli and Thermus thermophilus small ribosomal subunits: signatures of thermal adaptation." *PloS One,* vol. 8, no. 8, 5 Aug. 2013. https://doi.org/10.1371/journal.pone.0069898.
29. Hanwell, Marcus D, et al. "Avogadro: An Advanced Semantic Chemical Editor, Visualization, and Analysis Platform." *Journal of Cheminformatics*, vol 4, no. 1, 2012. https://doi.org/ 10.1186/1758-2946-4-17.
30. O'Boyle, Noel M, et al. "Open Babel: An Open Chemical Toolbox." *Journal of Cheminformatics*, vol. 3, no. 1, 7 Oct. 2011. https://doi.org/10.1186/1758-2946-3-33.
31. Neese, Frank. "The ORCA Program System." *WIREs Computational Molecular Science*, vol. 2, no. 1, 2011, pp. 73–78. https://doi.org/10.1002/wcms.81.
32. Trott, Oleg, and Arthur J Olson. "AutoDock Vina: improving the speed and accuracy of docking with a new scoring function, efficient optimization, and multithreading." *Journal of computational chemistry*, vol. 31, no. 2, 2010, pp. 455-61. https://doi.org/10.1002/jcc.21334.
33. Gill, Samuel C et al. "Binding Modes of Ligands Using Enhanced Sampling (BLUES): Rapid Decorrelation of Ligand Binding Modes via Nonequilibrium Candidate Monte Carlo." *The Journal of Physical Chemistry*, vol. 122, no. 21, 2018, pp. 5579-5598. https://doi.org/10.1021/acs.jpcb.7b11820.
34. Pettersen, Eric F et al. "UCSF Chimera-a visualization system for exploratory research and analysis." *Journal of*

https://doi.org/10.59720/22-241

Computational Chemistry, vol. 25, no. 13, 2004, pp. 1605-1612. https://doi.org/10.1002/jcc.20084.
35. The PyMOL Molecular Graphics System, Version 1.2r3pre, Schrödinger, LLC.